

# A Two-Moment Bulk Microphysics Scheme Coupled with a Mesoscale Model (WRF). Model Description and First Results

Wenhua Gao<sup>1</sup>, Fengsheng Zhao<sup>1</sup>, Zhijin Hu<sup>2</sup>, Xuan Feng<sup>1</sup>

<sup>1</sup>National Satellite Meteorological Center, Beijing, China

<sup>2</sup>Chinese Academy of Meteorological Sciences, Beijing, China

## Abstract

The Chinese Academy of Meteorological Sciences (CAMS) two-moment bulk microphysics scheme for mixed-phase clouds has been developed to improve the representation of cloud and precipitation processes. The proposed scheme predicts the mixing ratio of water vapor, the mixing ratios and number concentrations of five hydrometeor species (cloud droplets, rain, ice, snow, and graupel). A new parameterization approach to simulate the heterogeneous droplet activation is involved in the scheme, and a quasi-implicit integration method to effectively resolve the microphysical source and sink terms is also developed. Furthermore, the improved CAMS scheme has first been coupled with the Weather Research and Forecasting model (WRF v3.1), which makes it possible to simulate the microphysics of clouds and precipitation, as well as the cloud-aerosol interactions under relatively realistic atmospheric conditions.

A rain case occurring on 27-28 December 2008 in eastern China was simulated by using the coupled CAMS scheme and three sophisticated microphysics schemes in WRF model (i.e., Lin, Morrison, WDM6). Results show that the simulated 36-h accumulated precipitations are generally in agreement with the observations, and the CAMS scheme performs well in the south of the nested domain. The averaged precipitation intensity and hydrometeor mixing ratios simulated by the CAMS scheme are generally consistent with those of other microphysics schemes. The hydrometeor number concentrations simulated by the CAMS scheme are also close to the experiential values. The model results suggest that the CAMS scheme is basically reasonable and suitable in describing the microphysics of clouds and precipitation in the mesoscale model WRF.

Key words: Cloud Microphysics, Aerosol, WRF, CAMS, Coupling

## 1. Introduction

Cloud microphysical processes play an important role in the mesoscale and synoptic systems through affecting the thermodynamic structures of atmosphere, as well as the radiation fluxes of shortwave and longwave. Although numerous cloud microphysics schemes of varying degrees of sophistication have been developed and substantial improvements have been made over the past decades, our understanding of the microphysical processes remain one of the largest sources of uncertainty in NWP models. The bulk schemes represent the particle size with a distribution function, thus a limited number of parameters are required to describe the microphysical processes (Lin et al., 1983; Cotton et al., 1986; Tao and Simpson, 1993; Reisner et al., 1998; Morrison et al., 2005). As the computational advantage, the bulk microphysics schemes have been widely incorporated into the cloud-resolving models, mesoscale models, and climate models to simulate single clouds, mesoscale convective systems, precipitation processes, as well as atmospheric moisture and radiation budgets.

Recently, people are more interested in simulating the number concentration of each hydrometeor category, which

is a key variable in determining the cloud droplet effective radius and cloud optical thickness. The two-moment microphysics schemes, i.e., the mixing ratios and the number concentrations of hydrometeors are independently predicted, have gradually been implemented (Ziegler, 1985; Ferrier, 1994; Meyers et al., 1997; Cohard and Pinty, 2000; Morrison et al., 2005; Seifert and Beheng, 2006a, b; Hong and Lim, 2009). The particle number concentration influences the particle size, and then the terminal fall velocity, the microphysical structure (van den Heever and Cotton, 2004) and accumulated precipitation at the ground (Gilmore et al. 2004). In recent years, some advancements have been made to the two-moment schemes in terms of the aerosol inclusions and the use of lookup tables, and a number of the processes such as activation and collection can emulate bin-resolving schemes (Saleeby and Cotton, 2004; Seifert and Beheng, 2006a,b).

The Chinese Academy of Meteorological Sciences (CAMS) cloud microphysics scheme, a mixed-phase two-moment bulk scheme, was developed by Hu et al (1983, 1988). With some improvements in the past years, e.g., accurate calculation of supersaturation, reasonable representation of ice nucleation, detailed treatment of autoconversion, the scheme is more suitable to simulate the cloud microphysical processes. A new parameterization

approach of droplets nucleation is introduced into the CAMS scheme, which makes it possible to explore the effects of aerosol on clouds and precipitation. To advance the explicit representations of clouds and precipitation in the region of China, the improved CAMS scheme has been coupled with the Weather Research and Forecasting (WRF) model. A rain case is simulated to test the coupled CAMS scheme.

## 2. Bulk microphysics mesoscale model

### 1) NUCLEATION OF DROPLETS

More specific about the bulk cloud schemes is that only few of them carry a prognostic equation for the cloud droplet number concentration. The number of activated aerosols,  $N_{ccn}$ , is the number of dry aerosols which radius larger than the radius of smallest activated aerosol at a given supersaturation,  $S$ . Twomey's expression,  $N_{ccn} = c \cdot S^k$ , is usually accepted for  $S < 0.02\%$ , and which will overestimate the cloud droplet number concentration at high supersaturation (Cohard et al., 1998). An approach of aerosol activation similar to Abdul-Razzak et al. (1998) is developed in this scheme, which is performed for  $S > 0.02\%$ . Twomey's expression is used for  $S < 0.02\%$ , and it is also used to give the upper limit of activated aerosols for  $S > 0.6\%$ . A three-mode lognormal distribution of aerosol particles is adopted, and the size distribution parameters are from Hobbs (1993).

The scheme activates all previously unactivated aerosols with radius larger than a critical radius determined by the equilibrium theory (Stevens, 1996). The number of activated aerosols is obtained as Eq. (1).

$$N_{ccn} = \sum_{i=1}^3 \frac{N_{api}}{2} \left( 1 - \operatorname{erf} \left( \frac{\ln(r_{\min}/r_{mi})}{\sqrt{2} \ln \delta_i} \right) \right) \quad (1)$$

where  $N_{api}$ ,  $r_{mi}$ ,  $\delta_i$  are the total number concentration, geometric mean dry radius, and geometric standard deviation of aerosol mode  $i$ , respectively;  $r_{\min}$  is the dry radius of the smallest activated aerosol, which is determined by the calculated  $S$ . The actual activation number at each time step is determined by the difference between the number concentration of existing cloud droplets and the calculated  $N_{ccn}$ .

Kogan (1991) assumed that the condensation growth of aerosol particles with radius smaller than  $0.12 \mu m$  is

where  $\mathbf{V}$  is the 3D wind vector;  $v_M$  is the mass/number

$$\frac{\partial M}{\partial t} = -\mathbf{V} \cdot \nabla M + \frac{1}{\rho} \frac{\partial(\rho v_M M)}{\partial z} + D_M + \left( \frac{\partial M}{\partial t} \right)_{nuc} + \left( \frac{\partial M}{\partial t} \right)_{cond/evap} + \left( \frac{\partial M}{\partial t} \right)_{depo/subl} + \left( \frac{\partial M}{\partial t} \right)_{accr} + \left( \frac{\partial M}{\partial t} \right)_{freez/melt} + \left( \frac{\partial M}{\partial t} \right)_{auto} + \left( \frac{\partial M}{\partial t} \right)_{mult} \quad (3)$$

-weighted terminal fall velocity;  $\rho$  is the air density. The first three terms in the right hand of Eq. (3) represent the effects of advection, sedimentation, and turbulent diffusion.

based on the Kohler equation, while for larger ones the initial radius is less than the equilibrium radius. To consider the effects of larger aerosols, the aerosol particles with radius larger than  $0.12 \mu m$  are divided into 3 bins ( $0.12-1 \mu m$ ,  $1-5 \mu m$ ,  $>5 \mu m$ ) in this scheme, and a factor  $k$  ( $k = 7, 5, 5$ ) is introduced to calculate the initial sizes of the larger aerosols activated. The change in cloud water mixing ratio due to the droplet activation is then given by  $\Delta Q_{ccn} \approx \Delta N_{ccn} \times q_{c0} + \sum_{i=1}^3 N_{ccni} \times q_{ci}$ , where  $q_{c0}$  is the mass of the smallest cloud droplet,  $N_{ccni}$  is the number concentration of the activated droplets in  $i$  th bin,  $q_{ci}$  is the initial mass of the activated droplets in  $i$  th bin.

### 2) EQUATIONS OF CLOUD MICROPHYSICS

The improved CAMS microphysics scheme contains 5 classes of hydrometeors and 34 detailed processes of cloud microphysics. A total of 11 microphysical variables including the mixing ratio of vapor ( $q_v$ ), the mixing ratios and number concentrations of cloud droplets ( $q_c, N_c$ ), rain ( $q_r, N_r$ ), ice crystal ( $q_i, N_i$ ), snow ( $q_s, N_s$ ), and graupel ( $q_g, N_g$ ) are predicted. The size distribution of each hydrometeor category is described by a gamma distribution form:

$$\frac{dN_i(D)}{dD} = N_{i0} D^\alpha \exp(-\lambda_i D) \quad (2)$$

where subscript  $i$  denotes the hydrometeor species;  $N_{i0}$  and  $\lambda_i$  are the intercept and slope parameters of each hydrometeor;  $\alpha$  is specified as 2, 1, 0 for cloud droplet, ice/snow, and rain/graupeil, respectively. The particle masses are assumed to have the form  $m_i(D) = A_i \cdot D^{B_i}$ , and the particle terminal fall velocities have the form of  $V_i(D) = a_i \cdot D^{b_i} \cdot (p_{suf}/p)^{c_i}$ , where  $p_{suf}$ ,  $P$  are the surface pressure and atmospheric pressure respectively. The values of  $A_i, B_i, a_i, b_i, c_i$  are specified based on the theoretical and experimental results. The mass/number-weighted mean terminal velocities of each hydrometeor species for the entire size distribution are employed when calculating the fallout fluxes.

The conservation equation of each prognostic variable ( $M$ ) is considered as:

The remainder terms in the right denote the processes of nucleation, condensation/evaporation,

deposition/sublimation, accretion, freezing/melting, autoconversion, and multiplication, respectively.

### 3) SUPERSATURATION

The changes of mass mixing ratios by condensation and deposition are represented as a function of saturation. The related equations were described in detail by Hu (1988). Thus the accurate treatment of supersaturation is quite important in high-resolution cloud microphysics schemes. Tao et al. (1989) improved a saturation adjustment scheme with the inclusion of an ice-phase that calculates the amount of condensation/deposition necessary to remove any supersaturated vapor, or the amount of evaporation/sublimation necessary to remove any subsaturation in the presence of cloud droplets/cloud ice. In this scheme, a quasi-implicit integration approach is developed, which does not have time step constraints for stability. The calculations with this approach are stable and economical.

### 4) ICE NUCLEATION

Most of the ice particles are formed via heterogeneous nucleation on insoluble ice nuclei at temperatures warmer than  $-40^{\circ}\text{C}$ . Classical theory supports that the number concentration of activated ice nuclei,  $N_{pvi}$ , is a function of temperature and vapor supersaturation over ice (Fletcher, 1962; Meyers et. al., 1992). Furthermore, according to the experiments in cloud chamber, the ice nucleation rate is also a function of temperature variety rate. Although many studies and experiments have been done, the parameterization of heterogeneous ice nucleation process is still difficult and remains uncertain under certain conditions.

$$N_{pvi} = \begin{cases} -N_{IN} B_{IN} \exp[B_{IN}(273-T)] \frac{1}{\rho} \frac{dT}{dt} \frac{(q_v - q_{si})^5}{(q_{sw} - q_{si})^5} & T \leq 0^{\circ}\text{C} \text{ and } \frac{dT}{dt} < 0 \\ 0 & T > 0^{\circ}\text{C} \text{ or } \frac{dT}{dt} \geq 0 \end{cases} \quad (4)$$

In terms of the experimental results in Beijing,  $N_{IN} = 6.53$ ,  $B_{IN} = 0.342$  are taken.

### 5) AUTOCONVERSION

The collision and coalescence of cloud droplets to form raindrops is parameterized based on the numerical simulation results of Berry (1968). The following equation of autoconversion of cloud droplets to rain is deduced, and the reasonable results were obtained in the simulation of convective and stratiform clouds by Hu (1979, 1983).

$$Acr = \begin{cases} 0.25 \cdot \rho^2 \cdot q_c^3 / (360 \rho q_c + 1.20 N_c / D_c) & F_c \geq 1 \\ 0 & F_c < 1 \end{cases} \quad (5)$$

where  $N_c$  and  $D_c$  are the number concentration and dispersion of the initial size distribution of cloud droplets, respectively; the value of  $D_c$  is consistent with the continental nature and is approximate constant with height (Martin et. al., 1994);  $F_c$  represents the broadness of cloud droplets spectrum.

The autoconversion process is mainly related to the

cloud droplets number and the cloud water mixing ratio. The simulated number concentration of cloud droplets, primarily derived from the aerosol activation, can be used to quantitatively investigate the effects of aerosols on clouds and precipitation formation (Albrecht, 1989). Gao (2008) explored the influences of continental and maritime clouds on the evolutions of cloud microphysics by using this cloud droplet activation scheme and autoconversion parameterization. The simulation results indicated that the rate of autoconversion cloud to rain in maritime convective clouds is almost four times than that in continental convective clouds.

The coupling of CAMS cloud scheme to the mesoscale model WRF V3.1 is already in use. The standard WRF codes for advection of scalars are employed. The temperature and moisture tendencies are also calculated in the integration process. Overall, the CAMS microphysics scheme cooperates well with other components in the WRF model and can accurately drives the modules such as dynamics, atmospheric radiation, and cumulus parameterization, etc.

## 3. Case study

### a. Case introduction and experimental design

The precipitation case occurring during the period of 27 to 28 December 2008 in the middle and lower reaches of the Yangtze River in China is chosen. It is a representative precipitation process of mixed-phase stratus clouds in eastern China in winter. At the 500 hPa height, a large-scale trough over the middle latitudes moves slowly towards the southeast coast, and a strong low pressure is located over the Japan Sea. The warm and moist air is continuously transported from the Bay of Bengal to the Yangtze River Basin. Meantime, a strong wind shear is present at the 850 hPa height in the middle and lower reaches of the Yangtze River. The observed 36-h precipitation amounts (Figure 1) are greater than 5 mm in most of the region. There exists a southwest-northeast oriented rain band involving several rainfall centers with the values exceeding 20 mm. The maximum 36-h accumulated precipitation is about 28.3 mm, and the center position is located at  $30.9^{\circ}\text{N}$ ,  $120.9^{\circ}\text{E}$ .

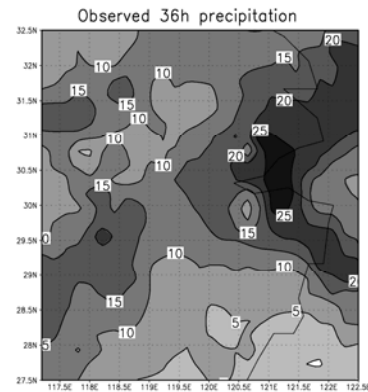


Figure 1. Observed 36-h accumulated precipitation (mm) from 0000 UTC 27 December 2008 to 1200 UTC 28 December 2008.

The coarse domain has  $180 \times 180$  points horizontally with a 9 km grid spacing. The nested domain has  $181 \times 181$  points horizontally with a 3 km grid spacing. The model is integrated for 36 hours with a time step of 54 s. The initial and lateral boundary conditions are taken from the NCEP analysis data. The RRTM and Dudhia scheme are used for the longwave and shortwave radiations. The Noah LSM is used for the land-surface process. The YSU planetary boundary layer parameterization with the M-O surface layer scheme is performed. The K-F cumulus parameterization is used only for the coarse domain. The coupled CAMS scheme is implemented in each domain to calculate the grid-scale precipitation, which is named as the exp-C experiment. To compare with other sophisticated microphysics schemes, the experiments by Lin (exp-L), Morrison (exp-M), and WDM 6-class (exp-W) schemes are also performed, respectively, under the same conditions

and designs.

### b. Results and analysis

Figure 2 shows the distributions of simulated 36-h accumulated precipitation over the nested domain. The distributions of simulated precipitation in the four experiments are generally in good agreement with the observations. However, the simulated maximum rainfall amounts are all more than the observations, and the positions of rainfall center are southerly a certain degree. Except for the exp-C experiment, the simulated rainfall amounts in the southwestern part of the nested domain are less than the observations about 5 mm. In addition, the simulations along the southeast coast of China in other two two-moment schemes (exp-M and exp-W) are some larger than the observations. Thus, the precipitation simulated by the CAMS scheme does well in the south of the nested domain.

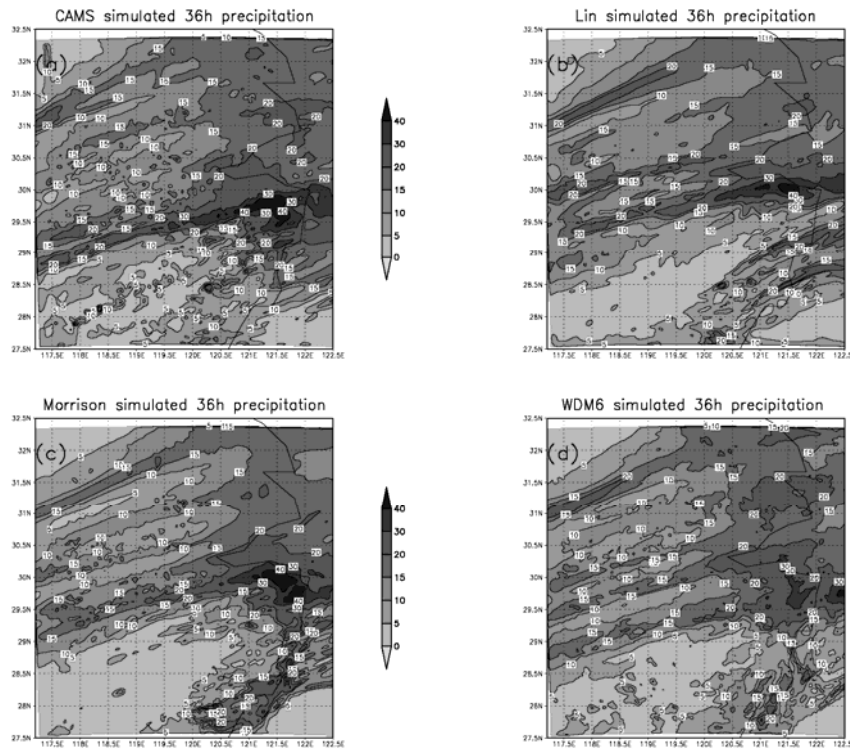


Figure 2. Simulated 36-h accumulated precipitation (mm) for the four experiments from 0000 UTC 27 December 2008 to 1200 UTC 28 December 2008. exp-C (a) exp-L (b) exp-M (c) exp-W (d).

To compare the precipitation rates, the time series of domain-averaged precipitation intensity are shown in Figure 3. A total of 148 auto-meteorological stations in the nested domain are chosen for calculating the average precipitation intensity. The start time of observation precipitation is about 0900 UTC 27, and the maximum precipitation intensity occurs during the period from 2300 UTC 27 to 0100 UTC 28. It is found that the evolutions of surface precipitation by the CAMS scheme generally agree

with those of other three microphysics schemes. The simulation precipitation intensities in the four experiments are some larger for the time periods of smaller precipitation rates, and the WDM6 scheme does a little better. The simulation results are some smaller and later around the time period of the precipitation maxima, and the CAMS scheme has better performance than others.

To investigate the capacity of CAMS scheme in simulating the cloud microphysics structure, the time

sequences of nested-domain mean vertical profiles of hydrometeor mixing ratios are shown in Figure 4. The graupel contents are quite small and are not plotted. The cloud water in the four experiments are mostly presented in warm regions (the zero degree isotherm is around 700 hPa layer). Some supercooled cloud droplets are found between 600hPa and 700hPa layers, and which are the most in the exp-M experiment. The maximum rain mixing ratios occur at 0100 UTC 28, and are one hour later than the cloud water. The maximum rain mixing ratio in the exp-W is approximately 0.12 g/kg, which is almost two times that of in other three experiments; however, the simulated precipitation intensity does not significantly increase. This is explained by more rain number concentration and then smaller rain size simulated in the WDM6 scheme. The simulated cloud water and rain water in the CAMS scheme are generally in agreement with those of in the Morrison and Lin schemes. The ice mixing ratio in exp-W experiment is the most in the four experiments, which occurs near the 350 hPa at 1200 UTC 27. There are two centers of ice mixing ratio in the exp-C experiment, one located at 350 hPa and another located at 600 hPa. These are just corresponding with the processes of nucleation and multiplication of ice at those layers. The snow mixing ratio in the exp-C experiment almost exceeds 0.15 g/kg and is the largest in the four experiments. The orders of hydrometeor mass evolution (i.e., ice→snow→cloud droplet/rain) reveal the development of cloud microphysical processes, which show the elementary feature of stratus cloud precipitation in winter.

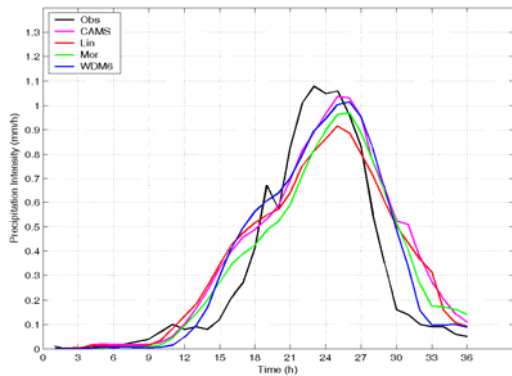


Figure 3. Time series of the surface precipitation intensity averaged in the nested domain.

The number concentrations of five hydrometeor species are explicitly predicted in the CAMS and Morrison schemes (cloud droplets number is not outputted in the Morrison scheme). All variables are averaged in the region of relatively larger precipitation ( $28.5^{\circ}$ - $30.5^{\circ}$  N,  $117.5^{\circ}$ - $119.5^{\circ}$ E) during the 36-h simulation period. The maximum number concentrations of rain in the exp-C and exp-M experiments are approximately  $0.5 g^{-1}$  and  $1.8 g^{-1}$ , respectively. The smaller autoconversion rate of droplets to

rain in CAMS scheme and the lower limit of rain diameter in Morrison scheme would be attributed to the difference. The maximum ice number concentration in the exp-M experiment is  $75 g^{-1}$ , which is about ten times that in the exp-C experiment. The parameterization of ice nucleation should be one of the major reasons for the difference. For example, when  $N_{IN} = 0.01$ ,  $B_{IN} = 0.6$  are taken (as Fletcher, 1962) in CAMS scheme, the simulated ice number concentration can increase by four times. This issue will be considered by numbers of observations in future parameterization development. The differences in snow and graupel number concentrations between the two schemes are relatively smaller. In addition, the maximum cloud droplets number concentrations in the exp-C and exp-W experiments are approximately  $4 \times 10^4 g^{-1}$  and  $8.3 \times 10^4 g^{-1}$ , respectively (in WDM6 scheme, only the cloud droplets and rain number concentrations are predicted). As a result, the big differences between the different schemes suggest that there still exist some uncertainty in simulating the hydrometeor number concentration, and which is one of the most difficult tasks in the development of cloud microphysics scheme.

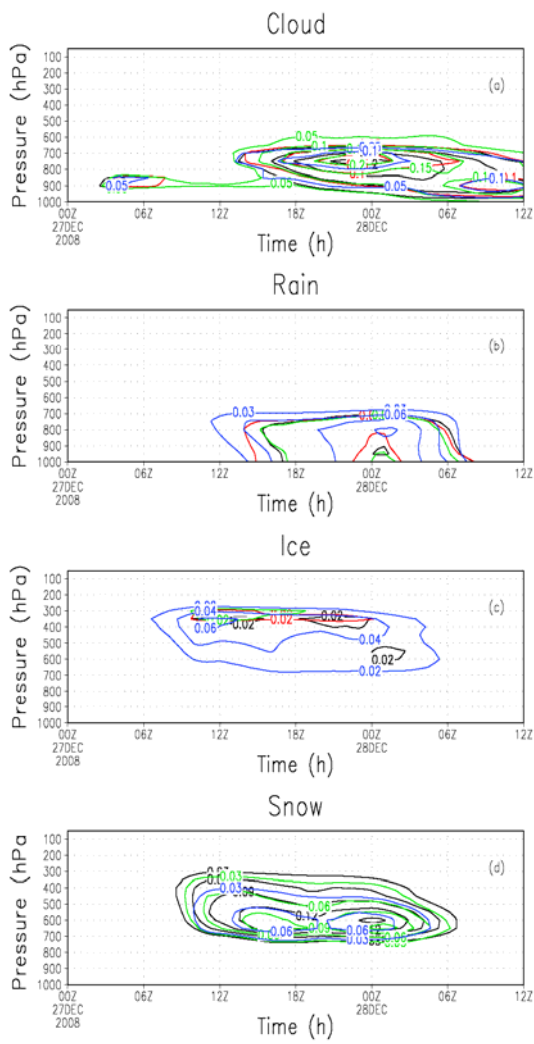


Figure 4. Time series of the four experiments simulated nested-domain mean vertical profiles of hydrometeor mixing ratios. exp-C (black), exp-L (red), exp-M (green), and exp-W (blue) experiments.

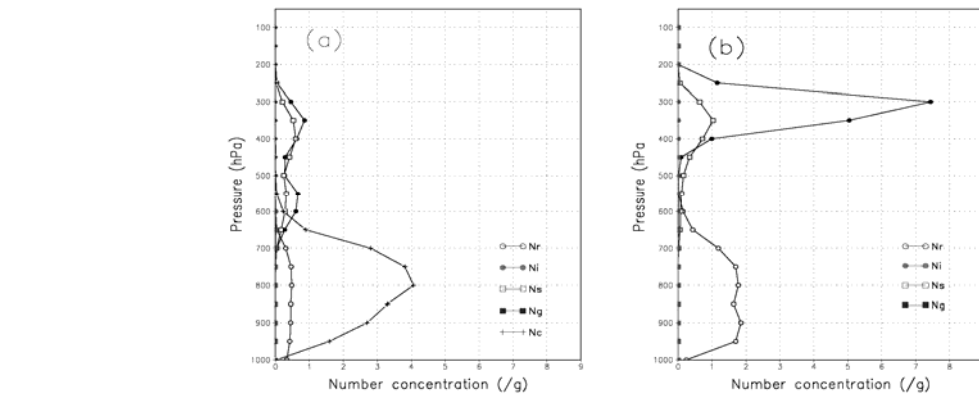


Figure 5. The vertical profiles of hydrometeor number concentrations averaged over the region (28.5°-30.5° N, 117.5°-119.5° E) during the 36-h simulation period in exp-C (a) and exp-M (b) experiments. (Units are  $10^4 \text{ g}^{-1}$  for cloud droplets,  $10 \text{ g}^{-1}$  for ice and snow, and  $1 \text{ g}^{-1}$  for rain and graupel).

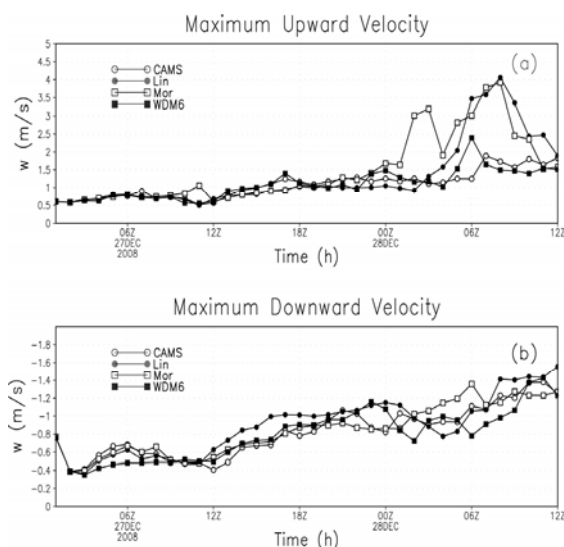


Figure 6. Time series of the four experiments simulated maximum upward velocity (a) and maximum downward velocity (b) in the nested domain.

Vertical velocity plays an important role in dominating the evolution of clouds. Since this is a case of stratus cloud precipitation, the vertical motion is relatively weaker. Fig.6 (a) illustrates that the maximum upward velocity in the exp-C experiment is generally in good agreement with that in the exp-W experiment. The simulation results in the four experiments in the time periods before 0000 UTC 28 are less than  $1.5 \text{ ms}^{-1}$ , but the differences are significant after 0200 UTC 28. The updraft velocities in the exp-M and exp-L experiments rapidly become stronger, which generally relates to the more latent heat resulting from the phase transfer processes. However, the mixing ratios of cloud water and cloud ice around the time periods of stronger updraft do not increase obviously. Perhaps the maximum upward velocities in the exp-L and exp-M experiments are somewhat inconsistent with the microphysical processes for lack of the prediction of cloud droplets number concentration (activated aerosols). In addition, the downward motion is primarily due to the falling of large particles. With the increase of updraft velocity, the corresponding downward velocity increases gradually and behaves similarly (Fig. 6b). In the mature and decaying stages of cloud development, the maximum upward velocities in the exp-C and exp-W experiments are slightly greater than the maximum downward velocities and are likely to be more reasonable.

#### 4. Summary

The CAMS two-moment bulk microphysics scheme has been described, and a new parameterization method has been included to simulate the heterogeneous cloud droplet activation. It provides a detailed treatment of cloud droplet activation by predicting the in-cloud supersaturation. Additional improvements are made in the following areas: 1) accurate calculation of supersaturation, 2) reasonable

representation of the ice nucleation, 3) detailed treatment of the autoconversion of cloud droplets to rain, etc. Then the improved CAMS scheme is coupled with the mesoscale model WRF V3.1, which makes it possible to simulate the microphysics of clouds and precipitation, cloud-aerosol interactions, as well as cloud optical properties under realistic atmospheric conditions.

A rain case in the period from 27 to 28 December 2008 in eastern China is simulated by using the coupled CAMS scheme and three sophisticated microphysics schemes in WRF model. Results show that the distribution of 36-h accumulated precipitation simulated by the CAMS scheme is generally in agreement with the surface observation, and it is better performance in the south of nested domain. The detailed comparisons reveal that the averaged precipitation intensity and mixing ratios of hydrometeor species simulated by the CAMS scheme are generally consistent with those of other three microphysics schemes. The number concentration of each hydrometeor type simulated by the CAMS scheme is also coincident with the number concentrations generally observed within stratus clouds. As a result, the CAMS scheme is basically reasonable and efficient in describing the microphysics of clouds and precipitation in the mesoscale model WRF.

#### References

- Abdul-Razzak, H., S.J. Ghan, and C. Rivera-Carpio, 1998: A parameterization of aerosol activation 1. Single aerosol type. *J. Geophys. Res.*, 103, 6123–6131.
- Albrecht, B. A., 1989: Aerosols, cloud microphysics, and fractional cloudiness. *Science*, 245, 1227–1230.
- Berry, E. X., 1968: Modification of the warm rain process. *Proc. 1st Nat. Conf., on Wea. Modif., Amer. Met. Soc., Albany, NY.*, 81–88.
- Cohard, J. M., J. P. Pinty, and C. Bedos, 1998: Extending Twomey's analytical estimate of nucleated cloud droplet concentration from CCN spectra. *J. Atmos. Sci.*, 55, 3348–3357.
- Cohard, J. M., and J. P. Pinty, 2000: A comprehensive two-moment warm microphysical bulk scheme. I: Description and tests. *Quart. J. Roy. Meteor. Soc.*, 126, 1815–1842.
- Cotton, W. R., G. J. Tripoli, R. M. Rauber, and E. A. Mulvihill, 1986: Numerical simulation of the effects of varying ice crystal nucleation rates and aggregation processes on orographic snowfall. *J. Climate Appl. Meteor.*, 25, 1658–1680.
- Ferrier, B. S., 1994: A double-moment multiple-phase four-class bulk ice scheme. Part I: Description. *J. Atmos. Sci.*, 51, 249–280.
- Fletcher, N. H., 1962: *Physics of rain clouds*. Cambridge University Press, p386.
- Gao, W. H., 2008: Numerical study of the effects of aerosols on clouds and precipitation. Doctoral dissertation, Chinese Academy of Sciences, Beijing, 77–80.
- Gilmore, M. S., J. M. Straka, and E. N. Rasmussen, 2004: Precipitation uncertainty due to variations in precipitation particle parameters within a simple microphysics scheme. *Mon. Wea. Rev.*, 132, 2610–2627.
- Hobbs, P.V., 1993: *Aerosol-Cloud-Climate Interactions*, Academic Press, Inc. P14.
- Hong, S.-Y., and K.-S. Lim, 2009: The WRF Double-Moment Cloud Microphysics Scheme (WDM). The 10th WRF User's Workshop, Boulder, U.S.A., 23–26 June.
- Hu Z. J., and L. Cai, 1979: A parameterized numerical simulation of warm rain and salt-seeding in cumulus clouds. *Scientia Atmospherica Sinica*, 3(4), 334–342. (in Chinese)
- Hu Z. J., C. Yan, and Y. Wang, 1983: Numerical simulation of rain and

- seeding processes in warm layer clouds. *Acta. Meteor. Sinica*, 41(1), 79-88. (in Chinese)
- Hu Z. J., and G. He, 1988: Numerical simulation of microphysical processes in cumulonimbus, Part 1: Microphysical model. *Acta Meteorologica Sinica*, 2(4), 471-489.
- Kogan, Y. L., 1991: The simulation of a convective cloud in a 3-D model with explicit microphysics. Part I: Model description and sensitivity experiments. *J. Atmos. Sci.*, 48, 1160-1189.
- Lin, Y.-L., R. D. Farley, and H. D. Orville, 1983: Bulk parameterization of the snow field in a cloud model. *J. Climate Appl. Meteor.*, 22, 1065-1092.
- Martin, G. M., D. W. Johnson, and A. Spice, 1994: The measurement and parameterization of effective radius of droplets in warm stratocumulus clouds. *J. Atmos. Sci.*, 51, 1823-1842.
- Meyers, M. P., P. J. Demott, and W. R. Cotton, 1992: New primary ice nucleation parameterization in an explicit model. *J. Appl. Meteor.*, 31, 708-721.
- Meyers, M. P., R. L. Walko, J. Y. Harrington, and W. R. Cotton, 1997: New RAMS cloud microphysics parameterization. Part II: The two-moment scheme. *Atmos. Res.*, 45, 3-39.
- Michalakes, J., and D. Schaffer, 2004: WRF Tiger Team Documentation: The Registry, available from : [http://www.mmm.ucar.edu/wrf/WG2/software\\_2.0/registry\\_schaffer.pdf](http://www.mmm.ucar.edu/wrf/WG2/software_2.0/registry_schaffer.pdf).
- Morrison, H., J. A. Curry, and V. I. Khvorostyanov, 2005: A new double-moment microphysics parameterization for application in cloud and climate models. Part I: Description. *J. Atmos. Sci.*, 62, 1665-1677.
- Reisner, J., R. M. Rasmussen, and R. T. Bruintjes, 1998: Explicit forecasting of supercooled liquid water in winter storms using the MM5 forecast model. *Quart. J. Roy. Meteor. Soc.*, 124, 1071-1107.
- Saleeby, S. M., and W. R. Cotton, 2004: Large-Droplet Mode and Prognostic Number Concentration of Cloud Droplets in the Colorado State University Regional Atmospheric Modeling System (RAMS). Part I: Module Descriptions and Supercell Test Simulations. *J. Appl. Meteor.*, 43, 182-195.
- Seifert, A., and K. D. Beheng, 2006a: A two-moment cloud microphysics parameterization for mixed-phase clouds. Part 1: Model description. *Meteorology and Atmospheric Physics*, 92, 45-66.
- Seifert, A., and K. D. Beheng, 2006b: A two-moment cloud microphysics parameterization for mixed-phase clouds. Part II: Maritime vs continental deep convective storms. *Meteor. Atmos. Phys.*, 92, 67-82.
- Stevens, B., G. Feingold, W. R. Cotton, and R. L. Walko, 1996: Elements of the microphysical structure of numerically simulated nonprecipitating stratocumulus. *J. Atmos. Sci.*, 53, 980-1006.
- Tao, W.-K., J. Simpson, and M. McCumber 1989: An ice-water saturation adjustment, *Mon. Wea. Rev.*, 117, 231-235.
- Tao, W.-K., and J. Simpson, 1993: The Goddard cumulus ensemble model, Part 1: model description. *Terr. Atmos. Oceanic Sci.*, 4, 35-72.
- van den Heever, S.C., and W.R. Cotton, 2004: The impact of hail size on simulated supercell storms. *J. Atmos. Sci.*, 61, 1596-1609.
- Ziegler, C. L. 1985: Retrieval of thermal and microphysical variables in observed convective storms. part I: Model development and preliminary testing. *J. Atmos. Sci.*, 42, 1487- 1509.

题目：双参数云微物理方案与WRF模式的耦合. 模式介绍及初步结果

作者：高文华<sup>1</sup>、赵凤生<sup>1</sup>、胡志晋<sup>2</sup>、冯绚<sup>1</sup>

单位：中国气象局国家卫星气象中心<sup>1</sup> 北京

中国气象科学研究院<sup>2</sup> 北京

关键字：云微物理、气溶胶、WRF、CAM5、耦合